*Progress In Electromagnetics Research, PIER 79, 251–262, 2008*

# ACCURATE MODELING OF MONOPOLE ANTENNAS IN SHIELDED ENCLOSURES WITH APERTURES

**X. C. Nie and N. Yuan**

Department of Electrical and Computer Engineering
University of Houston
4800 Calhoun Road, Houston, TX 77204, USA

**L. W. Li and Y. B. Gan**

National University of Singapore
10 Kent Ridge Crescent, Singapore 119260

**Abstract**—Monopole antennas are usually used for measurement of the shielding effectiveness of metallic enclosures. This paper presents an accurate numerical modeling for monopole antennas attached in shielded enclosures with apertures. The electric field integral equation (EFIE) is formulated for the induced currents on both the monopoles and enclosure. The precorrected-FFT accelerated method of moments (pFFT-MoM) is used to solve the integral equation and the incomplete LU (ILU) preconditioner is applied to speed up the convergence of the equation. Compared with existing methods, the model presented in this paper considers the mutual coupling between the monopoles and shielded enclosure. Therefore, it is a better approximation to the actual measurement geometry.

## 1. INTRODUCTION

Metallic shielding is usually used to prevent electronic equipments from electromagnetic interference. The shielding efficiency of a metallic enclosure is characterized by its shielding effectiveness (SE) [1–3]. For measurement of shielding effectiveness, small monopole antennas are usually used to penetrate the walls of the metallic enclosure and the voltages picked by the monopoles are measured. Shielding effective is then defined as the ratio of the voltage picked up by the monopole antenna without the presence of the enclosure to the voltage with the presence of the enclosure. Various methods have been developed to

determine the shielding effectiveness of metallic enclosures, such as the finite difference time domain (FDTD) method [4, 5], the method of moments (MoM) [6, 7] and the hybrid method [8]. Comparison with experimental data shows that it is far from easy to get accurate results and the memory requirements and computational complexity can be quite high, particularly at higher and resonant frequencies. Among the existing reference, most did not consider the monopole antenna. Others only considered simple dipoles located at the centre or outside the shielded enclosure. In these cases, the coupling between the dipole and enclosure is very weak and thus can be ignored [7]. All these simulation models are different from the actual measurement geometry, therefore may result in obvious discrepancy between the simulated and measured results.

In this paper, a model which is supposed to be a better approximation to the actual measurement geometry will be presented. A small monopole antenna is assumed to be attached on the internal surface of the metallic enclosure. Apertures are located on the wall of the enclosure for cooling purpose and cable connections. The mutual coupling between the monopole and enclosure may be very complicated and modify both the input impedance and induced current of the monopole antenna. For accurate analysis of such a model, a full-wave method is a good choice since it can fully consider the mutual coupling effect. We use the electric field integral equation (EFIE) to solve this problem. In the approach, the EFIE is set up on the surface of both the metallic monopole and enclosure. Then the method of moments (MoM) is used to solve the EFIE and the precorrected-FFT (pFFT) method [9] is applied to reduce the memory requirement and accelerate the matrix-vector products in the iterative solution of the equation. The incomplete LU (ILU) preconditioner [10] is applied to further improve the efficiency of the method by improving the convergence rate of the system. The resultant method can accurately predict the behaviour of the monopole antennas in the presence of the enclosure. Therefore, the shielding effectiveness of the enclosure can be accurately evaluated. The present method also enables the analysis of antennas in electrically large and complex enclosures due to the use of the fast algorithm.

## 2. SIMULATION MODEL AND FORMULATIONS

### 2.1. Simulation Model and the Integral Equation

Shielding effectiveness is usually measured around the internal surface of the enclosure by means of small monopoles penetrating the walls [11]. We use the model in Fig. 1 to simulate the measurement structure,

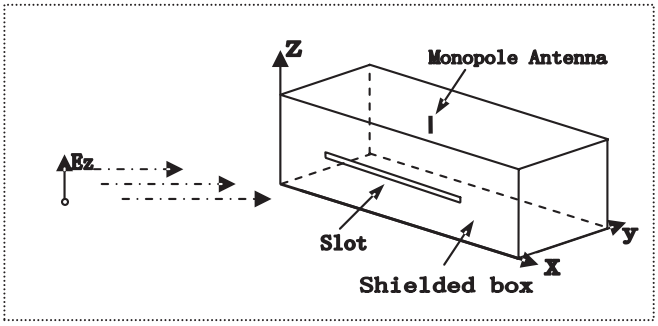


**Figure 1.** The geometry of a monopole enclosed by a shielded box with a slot.

a monopole antenna is attached in the perfectly-electrical-conducting (PEC) box with slots. Introducing equivalent surface current $\boldsymbol{J}_S$, wire current $\boldsymbol{J}_W$ and junction current $\boldsymbol{J}_J$ on the surface of the box, monopole antenna and their junction respectively, we can obtain the following integral equation:

$$\boldsymbol{E}^i_{\tan} = -\boldsymbol{E}^s_{\tan} \quad \text{on } S_S \text{ and } S_W \tag{1}$$

where $S_S$ and $S_W$ are the surfaces of the box and antennas, respectively. The scattered field $\boldsymbol{E}^s$ is the total contribution of $\boldsymbol{J}_S, \boldsymbol{J}_W$ and $\boldsymbol{J}_J$, which can be obtained from

$$\boldsymbol{E}^S(\boldsymbol{r}) = \sum_{\alpha}(-j\omega\boldsymbol{A}_\alpha(\boldsymbol{r}) - \nabla\Phi_\alpha(\boldsymbol{r})) \quad \alpha = S, W, J \tag{2}$$

where $\boldsymbol{A}_\alpha(\boldsymbol{r})$ and $\Phi_\alpha$ are the vector and scalar potential produced by the current $\boldsymbol{J}_\alpha$. Definitions of the vector and scalar potentials can be found in [12]. Introduction of the junction current $\boldsymbol{J}_J$ can model the rapidly varying surface current near the connection point and account for the continuity of electrical current from the monopole antenna to the box.

To solve Eq. (1), the conducting surface and wire are divided into triangular patches and linear segments, respectively. It should be noted that in meshing the structures, the junction point should be a vertex of the triangles in order to apply the attachment mode. Then the surface, wire and junction current are expanded using the Rao-Wilton-Glisson (RWG) basis function [13], triangular basis function [14] and junction basis function [14], respectively,

$$\boldsymbol{J}_\alpha(\boldsymbol{r}) = \sum_{n=1}^{N_\alpha} I^\alpha_n \boldsymbol{f}^\alpha_n(\boldsymbol{r}), \quad \alpha = S, W, J \tag{3}$$

where $N_S$, $N_W$ and $N_J$ are the numbers of unknowns on the surface (box), wire (monopole antennas) and junctions, respectively. Substituting (3) into (1), and using the Galerkin's method, we obtain a matrix equation in the following form

$$\begin{bmatrix} \boldsymbol{Z}^{S,S} & \boldsymbol{Z}^{S,W} & \boldsymbol{Z}^{S,J} \\ \boldsymbol{Z}^{W,S} & \boldsymbol{Z}^{W,W} & \boldsymbol{Z}^{W,J} \\ \boldsymbol{Z}^{J,S} & \boldsymbol{Z}^{J,W} & \boldsymbol{Z}^{J,J} \end{bmatrix} \begin{bmatrix} \boldsymbol{I}_S \\ \boldsymbol{I}_W \\ \boldsymbol{I}_J \end{bmatrix} = \begin{bmatrix} \boldsymbol{V}_S \\ \boldsymbol{V}_W \\ \boldsymbol{V}_J \end{bmatrix} \tag{4}$$

Elements of the sub-matrices $\boldsymbol{Z}^{\beta,\alpha}$ $(\beta, \alpha = S, W, J)$ are given by

$$Z_{mn}^{\beta,\alpha} = j\omega \int_{S_m^\beta} \boldsymbol{f}_m^\beta \cdot \boldsymbol{A}_{mn}^\alpha d\beta - \int_{S_m^\beta} \Phi_{mn}^\alpha \nabla_s \cdot \boldsymbol{f}_m^\beta d\beta \tag{5}$$

where $\boldsymbol{A}_{mn}^\alpha$ and $\Phi_{mn}^\alpha$ are the contributions to $\boldsymbol{A}$ and $\Phi$ from a single basis function $\boldsymbol{f}_n^\alpha$. The right-hand-side vector $\boldsymbol{V}$ in Eq. (4) is the excitation of the antenna-box system. For radiation mode, a 1 V-delta voltage is assumed at the connection point of the antenna and box. For receiving mode, $\boldsymbol{V}$ can be obtained by the reaction of the testing function $\boldsymbol{f}_m^\beta$ and the incident field, i.e.,

$$V_\beta = \int_{S_m^\beta} \boldsymbol{f}_m^\beta(\boldsymbol{r}) \cdot \boldsymbol{E}^i(\boldsymbol{r}) d\boldsymbol{r}, \quad \beta = S, W, J. \tag{6}$$

## 2.2. The Precorrected-FFT Method

By solving Eq. (4), the unknown coefficients are obtained, from which the shielding effectiveness of the shielded box can be calculated. However, the coefficient matrix $\boldsymbol{Z}$ is a dense and complex valued matrix, requiring $O(N^2)$ storage, where $N$ $(N = N_S + N_W + N_J)$ is the number of unknowns. A direct solution to Eq. (4) requires $O(N^3)$ operations and an iterative solution requires $O(N^{iter}N^2)$ operations, where $N^{iter}$ is the number of iterations required to satisfy a predefined convergence criterion. Such requirements are computational expensive and easily exceed the current capacity of a computer. To alleviate this problem, we use the precorrected-FFT (pFFT) method to reduce the memory requirement and speed up the matrix-vector products in the iterations.

The pFFT method considers the near- and far-zone interactions separately when evaluating a matrix-vector product, i.e.

$$\boldsymbol{Z} \cdot \boldsymbol{I} = \boldsymbol{Z}^{near} \cdot \boldsymbol{I} + \boldsymbol{Z}^{far} \cdot \boldsymbol{I} \tag{7}$$

The near-zone interactions are computed directly and stored while the far-zone interactions are calculated in an approximation way.

First, a uniform grid is introduced to enclose the entire solution domain, including the antennas and shielded box. Then, by matching the scalar or vector potentials produced by the source distributions ($\boldsymbol{f}_n^\alpha(\boldsymbol{r})$ and $\nabla \cdot \boldsymbol{f}_n^\alpha(\boldsymbol{r})$ $\alpha = S, W, J$) on the original irregular mesh and that produced by the grid sources at some pre-selected test points, we can construct the projection operators

$$\boldsymbol{W}^\alpha = \left[\boldsymbol{P}^{gt}\right]^+ \boldsymbol{P}^\alpha, \quad \alpha = S, W, J \tag{8}$$

where $\boldsymbol{P}^{gt}$ are the mappings between the grid sources and the test-point potentials, and $\boldsymbol{P}^\alpha$ are the mappings between the actual source distributions and the test-point potentials, respectively.

From the projection operators in Eq. (8), we can replace the original source distributions on the irregular mesh by a set of equivalent point sources on the uniform grid. Thus the relationship between the potentials at the grid points and the grid sources is in fact a convolution, which can be rapidly calculated by using the discrete Fast Fourier Transform (FFT). Once the grid potentials are obtained, the potentials on the original elements can be obtained via interpolation. The transpose of the projection operators can be used as the interpolation operators. Finally, the errors introduced into the nearby interactions by the grid approximation should be removed. Then the sub-matrix elements obtained by the pFFT method can be represented by the following formula

$$\hat{\boldsymbol{Z}}^{\beta,\alpha} = \widetilde{\boldsymbol{Z}}^{\beta,\alpha} + \left(\boldsymbol{Z}^{\beta,\alpha} - \boldsymbol{W}^{\beta \boldsymbol{T}} \boldsymbol{H} \boldsymbol{W}^\alpha\right), \quad \alpha, \beta = S, W, J \tag{9}$$

where $\boldsymbol{H}$ represents the convolution operators. The second term in the right-hand side of Eq. (9) is the so-called precorrection operator. It is required only when the distance between the basis function $\boldsymbol{f}_n^\alpha$ and the testing function $\boldsymbol{f}_m^\beta$ is less than a predefined threshold, otherwise, it is set to zero.

By using the above three sparse operators (projection, interpolation and precorrection) and one global operator (convolution), the matrix-vector multiply is sped up significantly and the memory requirement is also reduced. Detailed description about the implementation and efficiency of the pFFT method can refer to [9].

### 2.3. Incomplete LU Preconditioner

As we know, the EFIE usually converges slow, particularly at or around resonance frequencies. Since the CPU time is proportional to the required iteration number $N^{iter}$, preconditioning techniques should

be used to accelerate the convergence rate of the iterative solution [10, 15, 16]. In this paper, an incomplete LU preconditioner (ILU) with a dual dropping strategy [10] is used.

By using the ILU preconditioning, we construct a preconditioner $[\hat{\boldsymbol{Z}}]^{-1}$ from the incomplete LU factorization of the near-interaction part of the matrix $\boldsymbol{Z}$ and apply the preconditioner $[\hat{\boldsymbol{Z}}]^{-1}$ to Eq. (4). That is

$$\left[\hat{\boldsymbol{Z}}\right]^{-1} \boldsymbol{Z}\boldsymbol{I} = \left[\hat{\boldsymbol{Z}}\right]^{-1} \boldsymbol{V} \tag{10}$$

Now, in stead of solving the linear systems in (4), we need to solve the equivalent linear systems in (10), which usually converges much faster than the former.

The dual dropping strategy of the ILUT is implemented using the two parameters $\tau$ and $p$. The parameter $\tau$ means that small entries with respect to $\tau$ and relative to a certain norm of the current row are dropped and parameter $p$ means that the largest p entries are kept and the others are again dropped. By judicious choice of the parameters $\tau$ and $p$, we are able to construct an ILU preconditioner that is both effective and memory-saving. The efficiency of the ILU preconditioner will be shown in the next section.

## 3. EXAMPLES AND DISCUSSIONS

In the first example, we consider a monopole antenna mounted inside a rectangular shielded box with a rectangular slot at the centre of its front face, as shown in Fig. 1. The dimension of the box is 290 mm×190 mm×130 mm and the slot size is 150 mm×2 mm. The monopole antenna with a length of 65 mm is located at the centre of the top face of the box and terminated in a 50Ω load. The shielded box is normally illuminated by an external plane wave impinging on the surface of the enclosure ($x$-$z$ plane) with the electric field polarized along the $z$-axis. The shielding effectiveness is defined as follows by the voltages picked up by the monopole antenna instead of the electric field:

$$SE = 20 \log_{10} \frac{|V_i|}{|V_t|} \tag{11}$$

where $V_i$ and $V_t$ are the voltage picked up by the monopole antenna without and with the shielded box, respectively. For the case without the shielded box, only the monopole antenna and top face are considered.

In the calculation, the slotted box is discretized into 1352 triangles at the lower frequency end (0.5 GHz–1.5 GHz) and 4968 triangles at the higher frequency end (1.5 GHz–3 GHz). The monopole is divided

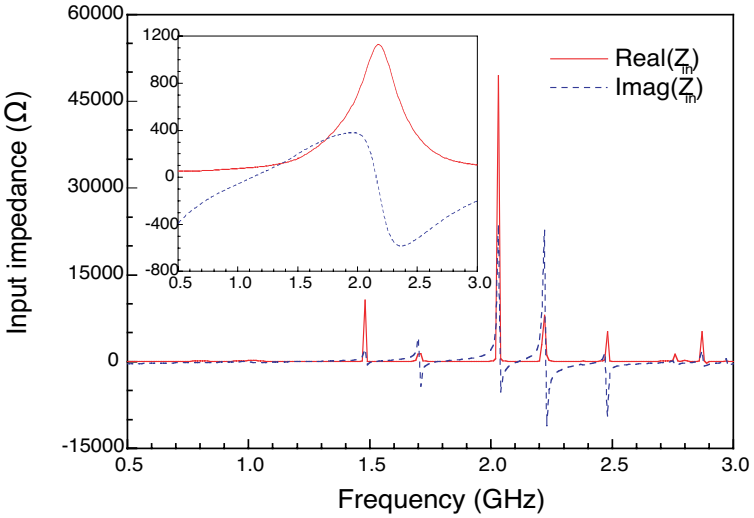


**Figure 2.** The input impedance of the monopole with and without (the inset) the shielded box.

into 8 segments. The numbers of unknowns for the lower and higher frequency end are 2026 and 7442, respectively. Fig. 2 shows the input impedance obtained from the present method over 0.5 GHz to 3 GHz (the frequency step is 0.01 GHz). For comparison, the input impedance without the shielded box is also shown in the inset of Fig. 2. It can be seen that the curves without the shielded box are very smooth. In contrast, the curves with the shielded box have a number of sharp peaks. These sharp peaks correspond to resonance frequencies of the shielded box.

Fig. 3 shows the current flowing through the junction point. From the currents, the voltages picked up the monopole antenna and the shielding effectiveness can be in turn calculated. Fig. 4 shows the shielding effectiveness obtained from the present method and FDTD method. Good agreement is observed, verifying the present method. In Fig. 4, the first wide valley around 1GHz is the resonance frequency of the slot. The first resonance frequency of the shielded box ($TE_{110}$ mode) near 0.94 GHz is suppressed by the resonance frequency of the slot and thus is not obvious. Other resonance frequencies ($TE_{111}$, $TE_{120}$ and $TE_{121}$ etc.) of the shielded box can be clearly observed in Fig. 4.

Finally, the shielding effectiveness of the same shielded box with slot of different sizes is calculated and shown in Fig. 5. The slots are of

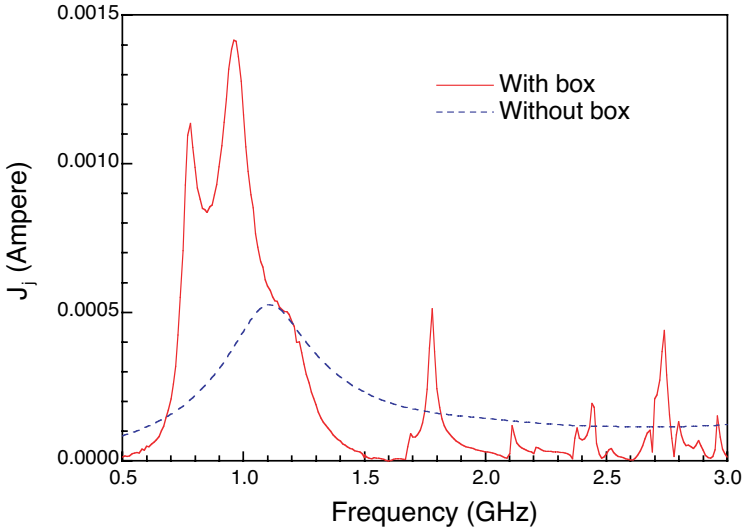


**Figure 3.** The magnitude of the electric current flowing through the junction point of the monopole with and without the shielded box.

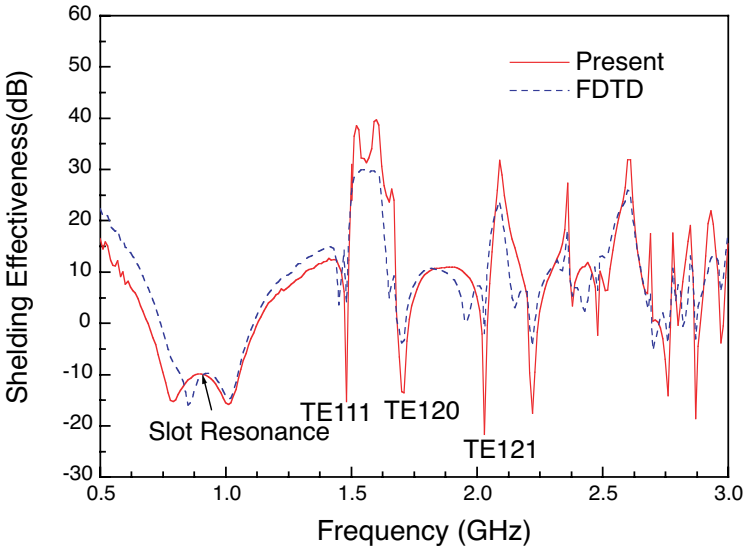


**Figure 4.** The shielding effectiveness of the shielded box.

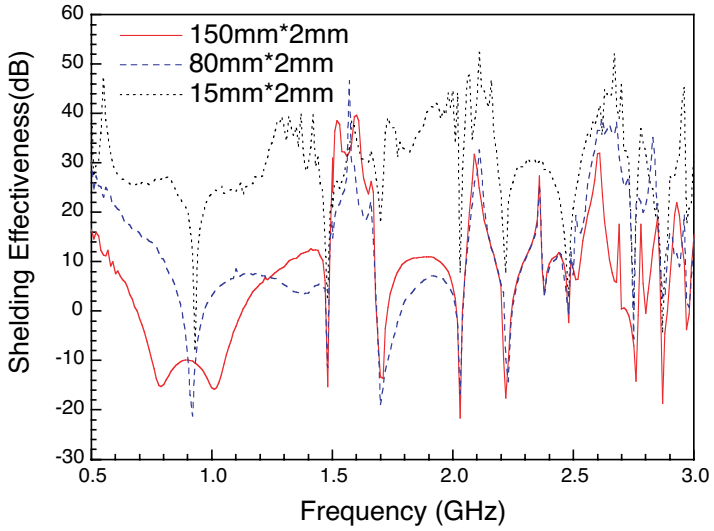


**Figure 5.** The shielding effectiveness of the shielded box with slots of different sizes.

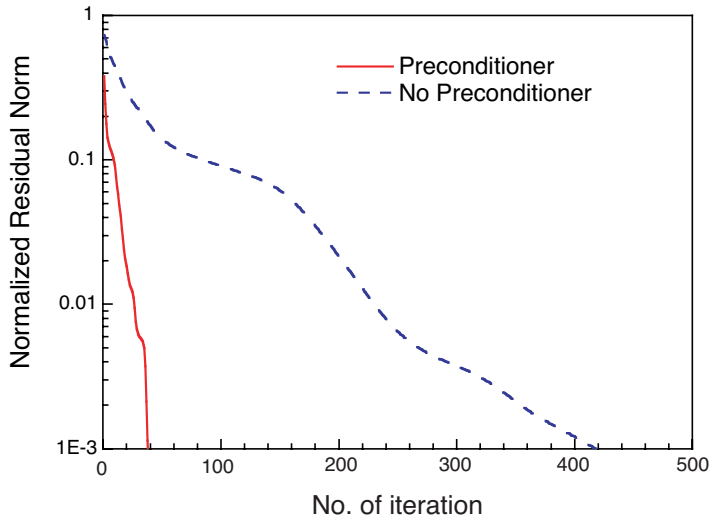


**Figure 6.** Convergence comparison of the system with and without ILU preconditioner.

three different sizes: 150 mm×2 mm, 80 mm×2 mm and 15 mm×2 mm. It is observed that the shielding effectiveness decreases as the slot size increases, especially at frequencies below the first resonance frequency. This phenomenon coincides with the physical principle (our expectation). Further, for shorter slots (80 mm and 15 mm), the resonance frequencies of the slots shift higher and is away from the first resonance frequency of the box (TE110 mode). Therefore, the $TE_{110}$ mode can be obviously observed from the curves for the two shorter slots.

To show the efficiency of the ILU preconditioner, Fig. 6 shows the convergence history of the system with and without preconditioner. It is seen that by using the ILU preconditioner, convergence can be achieved very fast. A relative residue of $10^{-3}$ can be achieved after only 39 iterations. However, if no preconditioner, the convergence is very slow. It takes about 420 iterations to achieve the same relative residue.

## 4. CONCLUSION

A model with better approximation to the actual measurement geometry of shielding effectiveness is presented in this paper. For accurate analysis of this model, the electric field integral equation is applied and the preconditioned-FFT method is used to reduce the memory requirement and CPU time. The incomplete LU (ILU) preconditioner is applied to further improve the efficiency of the method. Numerical results show that the present model and method are efficient in predicting the shielding effectiveness of metallic enclosures.

## ACKNOWLEDGMENT

The authors would like to thank Ms. Patricia, DSO National Laboratories of Singapore, for providing the results of the FDTD method.

## REFERENCES

1. Edrisi, M. and A. Khodabakhshian, "Simple methodology for electric and magnetic shielding effectiveness computation of enclosures for electromagnetic compatibility use," *Journal of Electromagnetic Waves and Applications*, Vol. 20, No. 8, 1051–1060, 2006.

2. Lei, J.-Z., C.-H. Liang, and Y. Zhang, "Study on shielding effectiveness of metallic cavities with apertures by combining parallel FDTD method with windowing technique," *Progress In Electromagnetics Research*, PIER 74, 82–112, 2007.
3. Wang, Y. J., W. J. Koh, and C. K. Lee, "Coupling cross section and shielding effectiveness measurements on a coaxial cable by both mode-tuned reverberation chamber and GTEM cell methodologies," *Progress In Electromagnetics Research*, PIER 47, 61–73, 2004.
4. Robinson, M. P., T. M. Benson, C. Christopoulos, J. F. Dawson, M. D. Ganley, A. C. Marvin, S. J. Porter, and D. W. P. Thomas, "Analytical formulation for the shielding effectiveness of enclosures with apertures," *IEEE Trans. Electromagn. Compat.*, Vol. 40, 240–248, Aug. 1998.
5. Li, M., J. L. Drewniak, R. E. Du Broff, T. H. Hubbing, and T. P. Van Doren, "EMI from cavity modes of shielding enclosures, FDTD modeling and measurements," *IEEE Trans. Electromagn. Compat.*, Vol. 42, 29–38, Feb. 2000.
6. Gerri, G., R. De Leo, and V. M. Primiani, "Theoretical and experimental evaluation of the electromagnetic radiation from apertures in shielded enclosures," *IEEE Trans. Electromagn. Compat.*, Vol. 34, 423–432, Nov. 1992.
7. Wallyn, W., D. D. Zutter, and H. Rogier, "Prediction of the shielding and resonant behavior of multisection enclosures based on magnetic current modeling," *IEEE Trans. Electromagn. Compat.*, Vol. 44, 130–138, Feb. 2002.
8. Feng, C. and Z. X. Shen, "A hybrid FD-MoM technique for predicting shielding effectiveness of metallic enclosures with apertures," *IEEE Trans. Electromagn. Compat.*, Vol. 47, 456–462, Aug. 2005.
9. Nie, X. C., L. W. Li, and N. Yuan, "Precorrected-FFT algorithm for solving combined field integral equations in electromagnetic scattering," *Journal of Electromagnetic Wave and Applications*, Vol. 16, No. 8, 1171–1187, Aug. 2002.
10. Saad, Y., "ILUT: a dual threshold incomplete LU factorozation," *Numer. Linear Algebra Appl.*, Vol. 1, No. 4, 387–402, 1994.
11. Paoletti, U., H. Garbe, and W. John, "Measurement of the shielding efficient of conducting enclosures with the image theory," *Advances in Radio Science*, Vol. 3, 137–142, 2005.
12. Yuan, N, X. C. Nie, Y. B. Gan, T. S. Yeo, and L. W. Li, "Accurate analysis of conformal antenna arrays with finite and curved frequency selective surfaces," *Journal of Electromagnetic*

*Waves and Applications*, Vol. 21, No. 13, 1745–1760, 2007.

13. Rao, S. M., D. R. Wilton, and A. W. Glisson, "Electromagnetic scattering by surfaces of arbitrary shape," *IEEE Trans. Antennas Propagat.*, Vol. 30, No. 3, 409–418, May 1982.
14. Hwu, S. U., D. R. Wilton, and S. M. Rao, "Electromagnetic scattering and radiation by arbitrary conducting wire-surface configuration," *IEEE APS Int. Symp. Dig.*, 890–893, 1988.
15. Wei, X. C., E. P. Li, and C. H. Liang, "Fast solution for large scale electromagnetic scattering problems using wavelet transform and its precondition," *Progress In Electromagnetics Research*, PIER 38, 253–267, 2002.
16. Wang, H. G., C. H. Chan, L. Tsang, and K. F. Chan, "Mixture effective permittivity simulations using IMLMQRF method on preconditioned EFIE," *Progress In Electromagnetics Research*, PIER 57, 285–310, 2006.